Effect of Ti_3AlC_2 particles on microstructure and tribological properties of micro-arc oxidation layer on TC4 alloy

Q. Li, J. Shang*, G. Y. Gu
Liaoning University of Technology, Jinzhou, 121000, Liaoning Province, China

TiO_2 metal oxide layers rich in Ti_3AlC_2 phase was successfully prepared on TC4 alloy by micro-arc oxidation (PECC or ASD) process. Analysis of the material phases contained in the PECC layer by X-ray diffractometry; scanning electron microscopy and energy spectroscopy were used to analyses the pores and elemental distribution on the surface of the specimens; the cross-sectional thickness of PECC layers were measured by metallographic microscope; confocal microscopy was used to measure the surface roughness of the sample; High temperature wear resistance of PECC layers with different Ti_3AlC_2 concentration was compared by tribological wear testing. The results show: 1) The incorporation of Ti_3AlC_2 particles plays an obvious catalytic role in the growth of PECC layer and the thickness is up to 74.74 μm; 2) When the concentration of Ti_3AlC_2 gradually increases, the PECC layers fluctuates obviously, and the deposition sealing effect is remarkable; 3) When the concentration is 4-6 g/L, the alloy has the best wear resistance, volume wear is only 1.98×10^{-4} $mm^3/N\cdot m$. Experiments have shown that surface modification of the alloy using the PECC process can further broaden the application of the alloy in the field of anti-wear.

(Received January 14, 2024; Accepted April 13, 2024)

Keywords: Micro arc oxidation, Titanium alloy, Tribology

1. Introduction

Titanium alloy [1,2] is an alloy composed of titanium and other elements, and its density is about 4.5 g/cm^2. Compared with other alloys, titanium alloys have broad application prospects in aerospace, marine and power engineering on account of their high specific strength [3-5]. Considering that the alloy has poor high temperature wear resistance in the long-term service environment [6], the effective life reduction rate is high. Therefore, many researchers have tried to use electroplating, diffusion metallizing, sol-gel synthesis and other methods [7-9] to strengthening wear resistance of alloys at high temperatures [10-12].

As a traditional process of metal surface modification, micro-arc oxidation technology [13] has been widely recognized because of its advantages of convenient operation, non-toxic and pollution-free, and short production cycle. The process is mainly to grow a layer of ceramic layer dominated by metal oxide on the surface of metal and its alloy in situ through the cooperation of electrolyte and electrical parameters. Studies have shown that the in-situ formed PECC layers can

* Corresponding author: shangbahao@163.com
https://doi.org/10.15251/DJNB.2024.192.593

be used as a protective layer for metals and their alloys to significantly optimize their surface properties [14-16]. However, considering that the metal oxide layer is involved in more reactions during the preparation process, the solid solution metal oxide is repeatedly broken down, melted and solidified, resulting in a large number of micropores and cracks in the oxide layer. Xu [17] added SiO_2 particles to the electrolyte, and found that most of the SiO_2 particles embedded on the PECC layer maintained a complete morphology and did not affect the original phase of the PECC layer. The appearance of SiO_2 nanoparticles can improve the hardness and wear resistance of the PECC layers to a certain extent, and reduce the growth defects of the PECC layers. Shokouhfar. [18] has compared the effect of different particles on the abrasion resistance of PECC layers concluded that the abrasion resistance of PECC layers after addition of different particles is TAO < TAO + Al_2O_3 < TAO + SiC < TAO + TiO_2. The addition of nanoparticles further improved the hardness of the PECC layer and reduced the surface roughness of the PECC layer, thus improving the tribological properties. Qingyuan et al. [19] Ti-6Al-4V is used as the experimental substrate to study the effect of graphene oxide particles with a concentration of 0-10 g/L on the microstructure and wear resistance of the PECC layer. The results showed that the layers thickness increased from 10 μm to 20 μm with the increase of graphene oxide particle concentration. When the addition amount was 5 g/L, friction coefficient decreased to the lowest value of 0.35.

In this experiment, under the premise of constant electrical parameters, 0,4,6,8 g/L Ti_3AlC_2 particles were added as experimental variables in the quantitative main salts. The microstructure and high temperature wear resistance of PECC layers prepared at different Ti_3AlC_2 particle concentrations were investigated. The purpose to find an excellent process to optimize the tribological properties of TC4 alloys.

2. Experimentation

TC4 alloys were used as the experimental substrate, and its size was φ25·4 mm. Before the experiment, sandpaper grinding, ultrasonic cleaning and acid-base cleaning were performed on the substrate. The PECC layers were prepared by WHD-30 micro-arc oxidation equipment, and the parameters were: constant current mode positive/negative current 1.5 A, 500 Hz, 15 min. The main salt system of the electrolyte was 8 g/L Na_2WO_4 + 6 g/L Na_2SiO_3 + 4 g/L Na_3PO_4, 0,4,6,8 g/L Ti_3AlC_2 particles were added in turn as experimental variables.

The SIGMA - 500 field emission scanning electron microscope (SEM) was used to observe the pore morphology on the surface of the specimen, and the porosity of the selected area was counted by Image J software. The surface element distribution of the sample was detected by surface scanning (EDS-map) using AZTEC X-Max spectrometer. The D/max-2500/pc type diffractometer (XRD) was used to detect the phase contained on the surface of the samples, and the obtained diffraction peaks were compared with the standard PDF card by Jade software. The surface flatness and wear width of the samples were observed by 3CCD confocal microscope. The thickness of PECC layer was measured by Axio Scope A1 metallographic microscope. The HT-100 friction tester was used to evaluate the wear resistance of the specimens. The test parameters were: high temperature 600 °C, external load 10 N, coupling time 10 min, and rotational speed 535 rpm. The data obtained were drawn by Origin software.

3. Results and analysis

From Fig.1 that when Ti_3AlC_2 particles are not added, there are a large number of pores similar to ' volcano ' on the PECC layer, and the number of large diameters micropores is large. When the addition amount of Ti_3AlC_2 increases to 4 g/L, PECC layers of surface has less deposits and the surface morphology tends to be flat. At the concentration of 6-8 g/L, PECC layers ' concave and convex ' undulates obviously. As Ti_3AlC_2 concentration increase, the surface morphology of the samples gradually approaches to the closed " concave and convex " undulating pore morphology from the porous " volcanic splash " morphology. It can be clearly seen from the ' black and white ' pore distribution that with the increase of Ti_3AlC_2 particle addition, pores proportion and pore size of PECC layers were obviously optimized. When the addition amount increased to 8 g/L, pores proportion and pore size of PECC layers were the lowest.

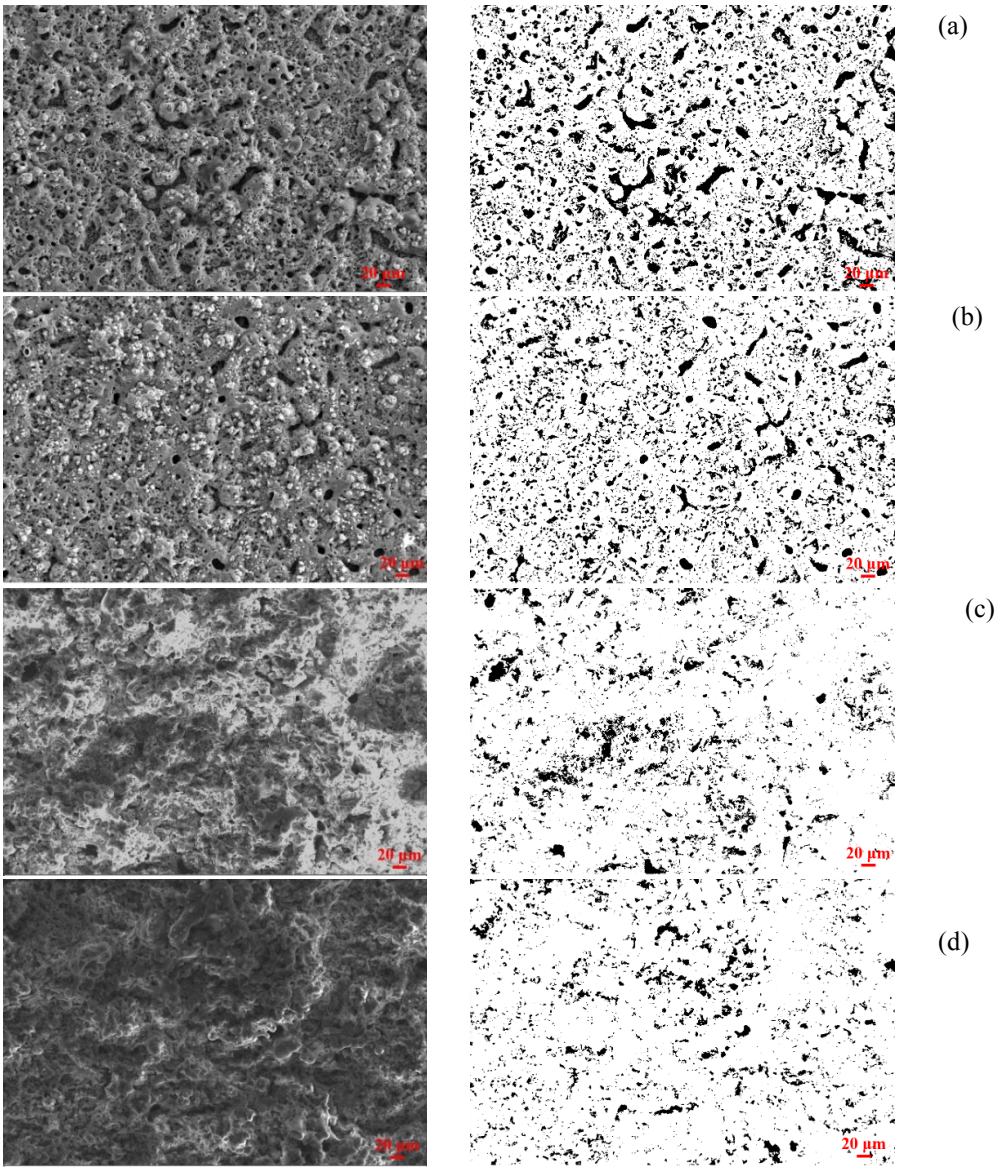

Fig. 1. Surface pore morphology of PECC layers, including, a: 0 g/L Ti_3AlC_2; b: 4 g/L Ti_3AlC_2; c: 6 g/L Ti_3AlC_2; d: 8 g/L Ti_3AlC_2

Flatness of the outer side of the microarc oxide layer is affected by particle deposition and field strength magnitude during the preparation process [20]. Among them, the evaluation of the flatness of the PECC layers mainly includes five parameters: Mean roughness Ra; maximum peak height R_p; maximum valley peak height R_v; average depression depth R_z; root mean square of depression R_q. From Figure that with the increase of Ti_3AlC_2 addition, the surface roughness of PECC layers decreases slightly and then increases. At Ti_3AlC_2 concentration of 4 g/L, the five parameters were the lowest and the flatness was the best.

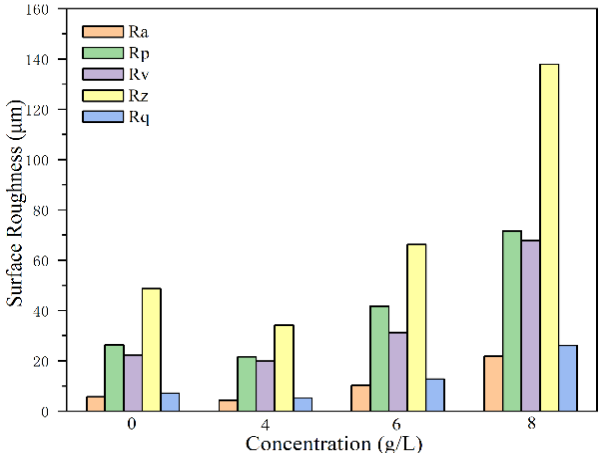

Fig. 2. Surface roughness of PECC layers

The cross-sectional thickness and surface porosity of PECC layers with different Ti_3AlC_2 additions were statistically analyzed, and Fig.3 was obtained. From the diagram, it can be seen that with the increase of Ti_3AlC_2 addition, the cross-sectional thickness of PECC layer shows an upward trend, and the surface porosity decreases significantly. The highest PECC layer thickness (74.74 μm) and the lowest porosity (8.07 %) were observed when the Ti_3AlC_2 concentration was 8 g/L. As a catalyst with good stability, Ti_3AlC_2 particles do not react with other substances in the electrolyte during the preparation of the layer. Therefore, as the reaction gradually participates in the layer growth, deposition and solidification in the PECC, the sprayed large holes are gradually repaired and play a certain ' sealing role '. On the other hand, Ti_3AlC_2 particles have conductivity. The addition of Ti_3AlC_2 particles to the solution changes the conductivity of the solution, optimizes the energy density during discharge, and improves the layer quality to a certain extent. At a concentration of 8 g/L, the most particles were deposited on the outside of the alloy, and the PECC layer was lifted and had the roughest surface. This is because the increase of Ti_3AlC_2 content in the electrolyte is involved in the growth of the film layers, and the Ti_3AlC_2 particles deposited and solidified in the PECC layer are increased. In the meantime, affected by the conductivity of the solution, the discharge energy is the most intense at this moment, resulting in a significant change in the flatness of PECC layers, which is also consistent with the conclusion of Fig.2.

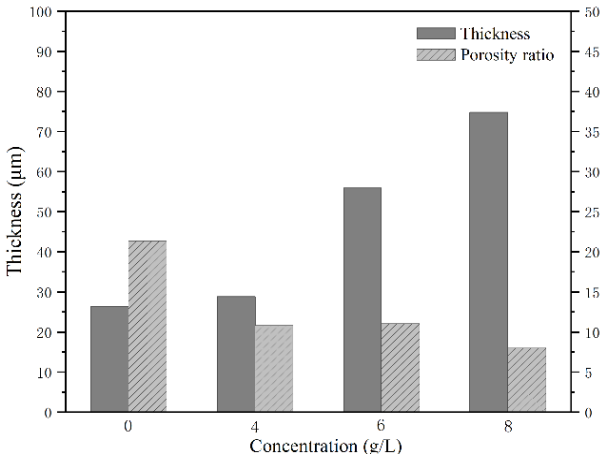

Fig. 3. Statistics of PECC layer thickness and porosity under different Ti_3AlC_2 additions.

Fig.4 shows the fluctuation of the response voltage of the PECC layers with time for different Ti_3AlC_2 concentrations. It can be seen from the Fig.4 that there is a significant difference in the breakdown voltage at the first stage of micro-arc oxidation (arcing stage). Amplifying this stage, it can be seen that as the Ti_3AlC_2 addition increase, the breakthrough voltage required for arcing stage of the PECC layer gradually increases. Especially when the concentration of is 6-8 g/L, arcing voltage increases significantly compared with 0 g/L. The change of arcing voltage is mainly due to the increase of Ti_3AlC_2 addition, which changes the conductivity of the solution. With the increase of Ti_3AlC_2 addition, the conductivity of the solution gradually increased. Therefore, With the positive increase of Ti_3AlC_2 concentration, the arcing voltage of PECC layers gradually increases, the energy carried by charged particles in the solution increases, and they transfer each other in the discharge channel between the substrate and the electrolyte. The sealing of Ti_3AlC_2 particles increases the transfer resistance of the particles, and the lifting of the molten product eventually leads to a decrease in surface flatness and an increase in thickness.

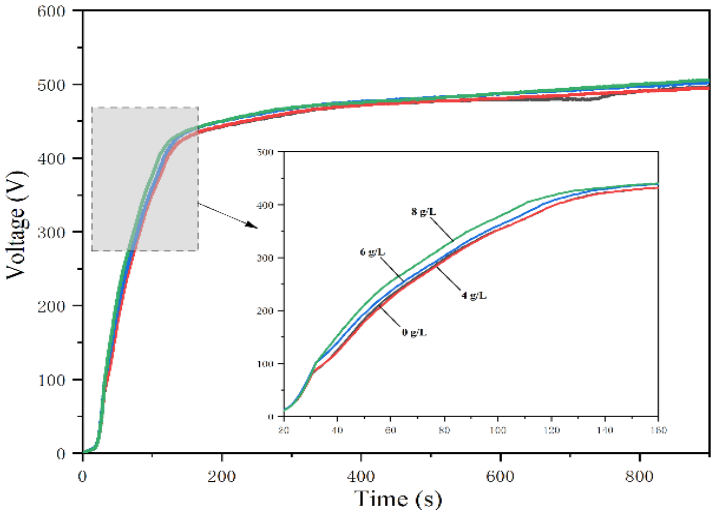

Fig. 4. The response of voltage with time under different Ti_3AlC_2 additions.

From Fig.5 that an insulating ceramic layer rich in Anatase-TiO_2, Rutile-TiO_2, Ti and Ti_3AlC_2 phases is formed on the surface of TC4 alloy after micro-arc oxidation. The diffraction peaks of Anatase-TiO_2 are mainly concentrated at 2θ = 25.33 °, 47.91 °, 82.84 °. Diffractive peaks Rutile-TiO_2 are concentrated at 2θ = 27.48 °, 36.06 °, 54.34 °. Diffractive peaks of Ti_3AlC_2 are concentrated at 2θ = 39.15, 41.74 °. From the diagram, at gradually increasing concentrations of Ti3AlC2 additions, diffractive peaks intensity of Anatase-TiO_2 gradually weakens. This is because the addition of Ti_3AlC_2 promotes the thermal conductivity of the electrolyte reaction, which makes the low-temperature Anatase-TiO_2 transform to the high-temperature Rutile-TiO_2. The intensity of Rutile-TiO_2 diffraction peak increased. As the Ti_3AlC_2 concentration increased to 8 g/L, the electrolyser was filled with a large number of Ti_3AlC_2 particles. Adequate Ti_3AlC_2 is deposited at the defects of PECC layers and accumulates with the growth of PECC layers. Therefore, when 2θ = 39.15 °, the diffraction peak of Ti_3AlC_2 reaches the strongest. This also indicates that the added Ti_3AlC_2 can be successfully deposited on the PECC layers.

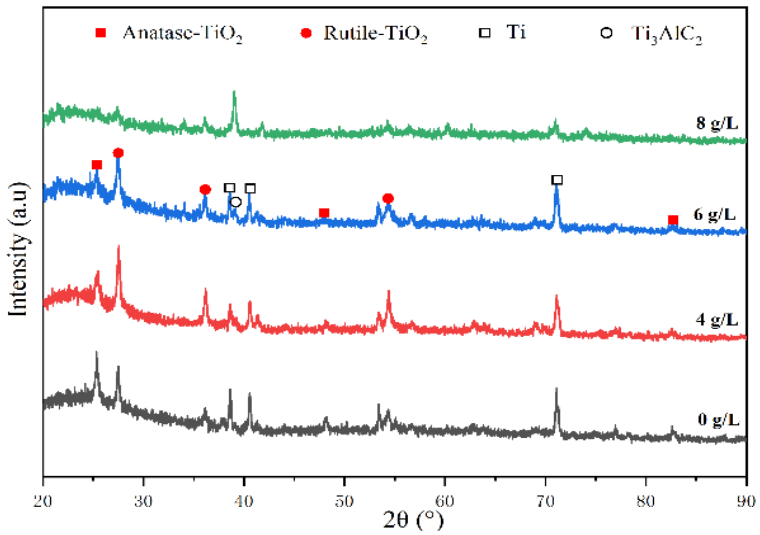

Fig. 5. X-ray diffraction peak of PECC layers

The PECC layers prepared at different Ti_3AlC_2 concentrations were analyzed by EDS-map, and Fig.6 was obtained. As can be seen from Fig.6, Na element at 0 g/L concentration is gradually replaced by Al element at gradually increasing Ti_3AlC_2 concentration. From the distribution of Ti and Al elements in the selected area of the samples, the bright area where Al is located overlaps with the area where Ti is located. This is mainly due to the fact that Ti_3AlC_2 particles maintain their aggregation state during the preparation of PECC layers. Therefore, the Ti element detected on the surface of the PECC layers not only comes from the base material and TiO_2, but also contains Ti in Ti_3AlC_2, so the bright area of the Al element on the surface of the sample overlaps with some Ti. Combined with the analysis of Fig.5, it is further proved that the added Ti_3AlC_2 particles are successfully attached to the PECC layers.

The high temperature wear resistance of PECC layers prepared at 4 groups of Ti_3AlC_2 concentrations were tested. The friction coefficient and friction wear are important indicators to measure the wear resistance of materials [21,22]. Many researchers divided the grinding stage into a) initial stage and b) stable stage according to the floating strength of the friction coefficient of the

two kinds of grinding materials with time [23,24]. Later, with the emergence of many surface treatment technologies for metals and their alloys, one or more layers of strengthening layers were grown on the surface of the substrate inward or outward. Therefore, the grinding stage is not limited to the above two stages.

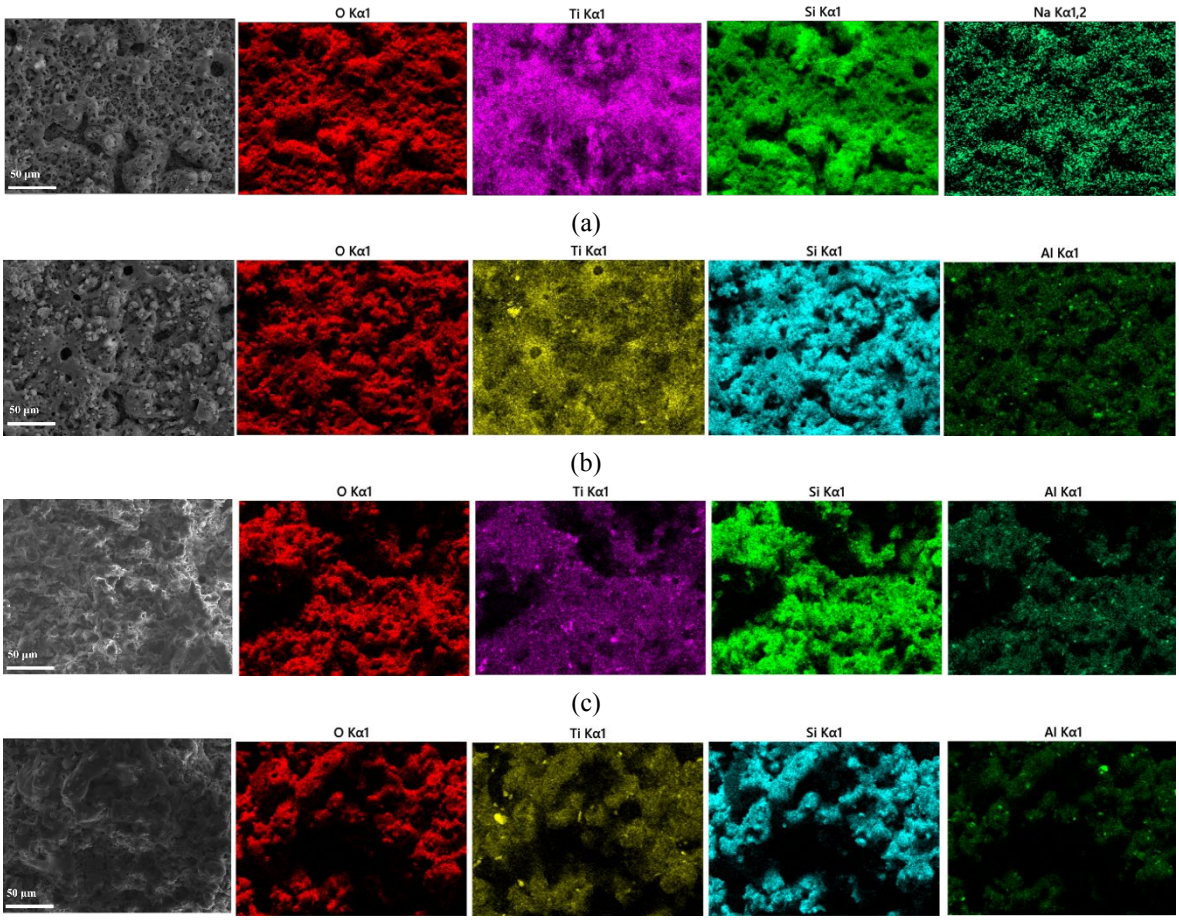

Fig. 6. EDS-map of PECC layers, including, a: 0 g/L Ti_3AlC_2; b: 4 g/L Ti_3AlC_2; c: 6 g/L Ti_3AlC_2; d: 8 g/L Ti_3AlC_2

From Fig.7 that PECC layers have obvious a) and b) stages during the friction and wear test. Because the PECC layer has excellent wear resistance, the in-situ grown metal oxide layer is not completely destroyed after high temperature grinding for 10 min. Therefore, the third stage of the dynamic friction coefficient change did not appear, which further confirmed that the TiO_2 oxide layer played an effective protective role in the substrate under the high temperature grinding environment. From figure that in the initial stage of grinding, with the increase of Ti_3AlC_2 addition, the surface flatness of the material tends to decrease. When the concentration of Ti_3AlC_2 reached 8 g/L, dynamic friction coefficient changes most prominently. When the two materials are in the stable stage of grinding, the dynamic friction coefficient of PECC layers prepared with Ti_3AlC_2 addition of 4 g/L tends to be stable and the lowest. This indicates that the addition of Ti_3AlC_2 under this condition promotes the more uniform distribution of TiO_2 in the layer as a self-lubricating phase on the substrate. When the concentration of Ti_3AlC_2 reaches 8 g/L, flatness

of the material surface is the lowest. In the process of grinding coupling, there are still some furrows remaining in the wear area, so the dynamic friction coefficient is the highest at this time.

Fig.8 shows the statistics of average friction coefficient and volume wear rate of PECC layers. From figure, it can be seen that when the concentration of Ti_3AlC_2 increases, the average friction coefficient and volume wear decrease first and then increase. Among them, at a concentration of Ti_3AlC_2 of 4 g/L, the average friction is lowest (0.429); At a concentration of Ti_3AlC_2 of 8 g/L, the average friction coefficient reaches the highest (0.488). This is also consistent with the analysis conclusion of Fig.7. From Fig.8 that without the addition of Ti_3AlC_2 particles, maximum wear rate is about 3.781×10^{-4} $mm^3/N\cdot m$; when the addition of Ti_3AlC_2 increased by 6 g/L, the volume wear rate reached the lowest, only 1.98×10^{-4} $mm^3/N\cdot m$. The average friction coefficient increased significantly when the addition of Ti_3AlC_2 was 6 g/L. This is due to the agglomeration of Ti_3AlC_2 particles and the low surface flatness. Under this condition, wear rate of PECC layer is lowest, which is caused by the uniform distribution of anti-wear phase. Combined with the friction coefficient and volume wear rate, it can be seen that when the content of Ti_3AlC_2 is 4-6 g/L, wear resistance of micro-arc oxide layer is the best.

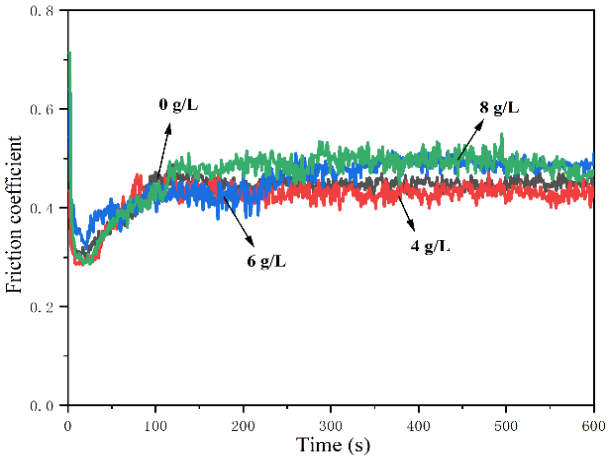

Fig. 7. Dynamic friction coefficient curve.

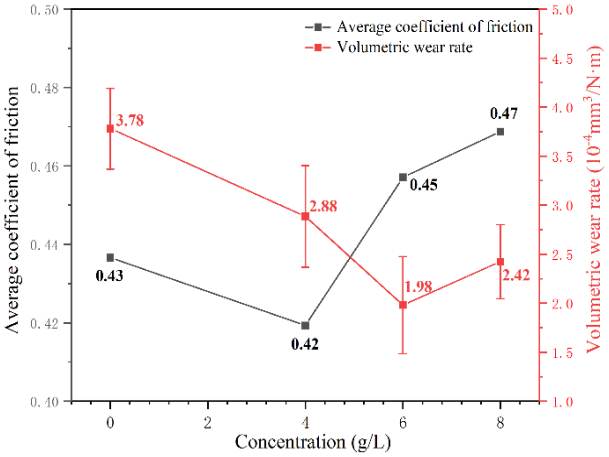

Fig. 8. Average friction coefficient and wear rate

Theoretically, lattice mismatch between Ti_3AlC_2 and TiO_2 is high. As shown in Fig.9, during the stacking process of TiO_2 melt, Ti_3AlC_2 is dispersed as a deposited particle at the interface of the melt stacking, so a non-coherent interface is formed at the interface between Ti_3AlC_2 and TiO_2 [25]. On the one hand, the incoherent interface can fill the pores of the layer's growth, hinder the dislocation movement of the TiO_2 lattice, reduce the lattice strain, and reduce the interplane free energy. On the other hand, it may cause moderate interfacial bonding strength. Combined with the growth thickness of the layer, it can be seen that this method of deposition dispersion leads to the obvious uplift of the layer at the incoherent interface, promotes the outward growth of the layer, and the macropores are gradually filled to ensure that TiO_2 can provide wear resistance for a longer period of time.

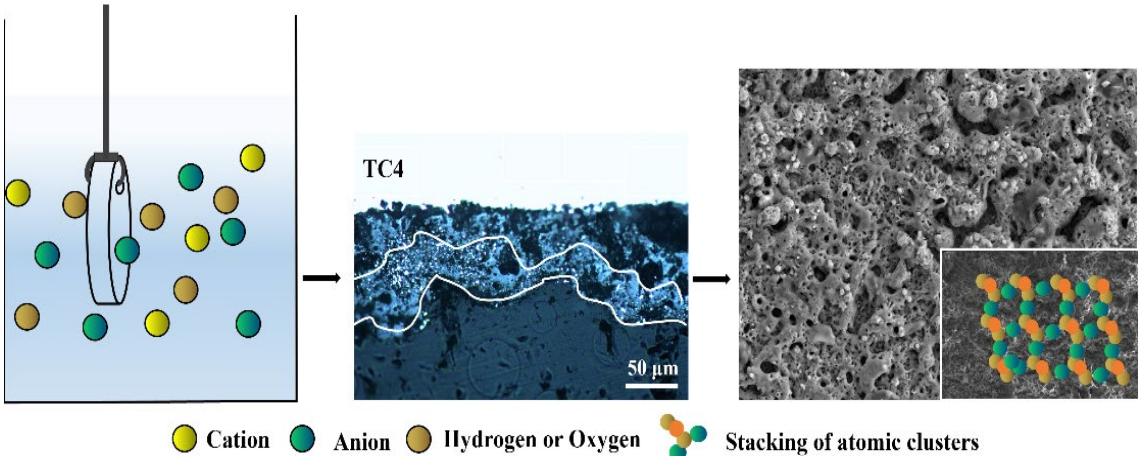

Fig. 9. Incoherent interface between Ti_3AlC_2 and TiO_2.

4. Conclusion

TiO_2 metal oxide layers rich in Ti_3AlC_2 phase was successfully prepared on TC4 alloy by micro-arc oxidation (PECC or ASD) process. The effect of Ti_3AlC_2 particles on the microstructure of PECC layer was investigated by adding 0,4,6,8 g/L Ti_3AlC_2 particles into the electrolyte as experimental variables. The tribological properties of PECC layers prepared at different Ti_3AlC_2 concentrations were evaluated.

The results show that as the Ti_3AlC_2 content increases, the surface roughness of PECC layers decreased. When the addition amount of Ti_3AlC_2 is 8 g/L, more Ti_3AlC_2 particles are deposited on the PECC layers, and the PECC layers appears uplift and the surface roughness increases. The concentration of Ti_3AlC_2 in the electrolyte has little effect on the phase composition of the PECC layer. Under the condition of different concentrations of Ti_3AlC_2, the micro-arc oxidation layer is mainly composed of TiO_2 and Ti phases, containing a small amount of Ti_3AlC_2 phase. With the increase of Ti_3AlC_2 concentration, the content of Ti_3AlC_2 phase in the PECC layers increases.

The wear resistance of PECC layer is closely related to the addition of Ti_3AlC_2 particles. When added at a concentration of 4 g/L, average friction coefficient is the lowest 0.419. When added at a concentration of 6 g/L, volume wear rate reaches the lowest, which is 1.98×10^{-4}

$mm^3/N \cdot m$. Comparing the surface morphology, phase composition and wear resistance of Ti_3AlC_2 particles with different concentrations, it is concluded that the optimum addition amount of Ti_3AlC_2 particles in the laboratory is 4-6 g/L.

Acknowledgement

The authors thank the Science and Technology Program of Liaoning Provincial Department of Education for its financial support for this research, the grant number is: JYTMS20230845.

References

[1] F. H. Froes, H. B. Bomberger, JOM. 37(1985)28–37; https://doi.org/10.1007/BF03259693
[2] Q. J. Wang, J. R. Liu, R. Yang, JAM. 34(4) (2014)1-26; https://doi: 10.11868/j.issn.1005-5053.2014.4.001
[3] A. Pathania, S. A. Kumar, B. K. Nagesha, S. Barad, T.N. Suresh, Mate. Today: Proc. 45(2021)4886-4892; https://doi:10.1016/j.matpr.2021.01.354
[4] Y. Li, Z.L. Zhou, Y.Y. He, Materials. 17(1) (2024)65; https://doi.org/10.3390/ma17010065
[5] A. Festas, A. Ramos, J.P. Davim, Proc Inst Mech Eng B J Eng Manuf. 236(4) (2022)309-318; https://doi:10.1177/09544054211028531
[6] R. R. Boyer, Mater. Sci. Eng. A. 213(1996)103-114; https://doi:10.1016/0921-5093(96)10233-1
[7] R. Sitek, J. Kaminski, J. Borysiuk, H. Matysiak, K. Kubiak, K.J. Kurzydlowski, Intermetallics. 36(2013)36-44; http://dx.doi.org/10.1016/j.intermet.2012.12.017
[8] O.A. Markelova, V.A. Koshuro, E.O. Osipova, A.A. Fomin, Metallurgist. 67(2023)338–343; https://doi.org/10.1007/s11015-023-01520-5
[9] X.J. Zhao, P.Z. Lyu, S.Q. Fang, S.H. Li, X.X. Tu, P.H. Ren, D. Liu, L.M. Chen, L.R. Xiao, S.N. Liu, Materials. 17(1) (2024)100; https://doi.org/10.3390/ma17010100
[10] A. Bloyce, P. Y. Qi, H. Dong, T. Bell, Surf. Coat. Technol. 107(2-3) (1998)125-132; https://doi:10.1016/s0257-8972(98)00580-5
[11] G. Hou, A. Li, Appl. Sci. 11(16) (2021)7471; https://doi.org/10.3390/app11167471
[12] D. He, S. Zheng, J. Pu, G. Zhang, L. Hu, Tribol Int. 82(2015)20-27; https://doi:10.1016/j.triboint.2014.09.017
[13] Q. Li, W. Yang, C. Liu, D. Wang, J. Liang, Surf. Coat. Technol. 316(2017)162-170; https://doi:10.1016/j.surfcoat.2017.03.021
[14] Y. Cheng, J. Cao, M. PECC, Z.M. Peng, P. Skeldon, G.E. Thompson, Surf. Coat. Technol, 269(2015) 74-82; https://doi:10.1016/j.surfcoat.2014.12.078
[15] M. Babaei, C. Dehghanian, M. Vanaki, App. Surf. Sci. 357(2015)712-720; https://doi:10.1016/j.apsusc.2015.09.059
[16] S. Durdu, M. Usta, App. Surf. Sci. 261(2012)774-782;

https://doi:10.1016/j.apsusc.2012.08.099
[17] G.Q. Xu, X.K. Shen, Surf. Coat. Technol. 364(2019)180-186;
https://doi.org/10.1016/j.surfcoat.2019.01.069
[18] M. Shokouhfar, S.R. Allahkaram, Surf. Coat. Technol. 309(2017)767-778;
https://doi:10.1016/j.surfcoat.2016.10.089
[19] Q.Y. Hu, X.M. Li, G. Zhao, Y.L. Ruan, G.Q. Wang, Q.J. Ding, Coatings. 13(2023)1-12;
https://doi.org/10.3390/coatings13111967
[20] G.Y. Gu, J. Shang, X.Y. Zhang, Chalcogenide Lett, 19(12) (2022)955-964;
https://doi.org/10.15251/CL.2022.1912.955
[21] P.J. Blau, Tribol Int. 34(9) (2001)585-591; https://doi:10.1016/s0301-679x(01)00050-0
[22] Kato, K. Wear, 241(2) (2000)151-157; https://doi:10.1016/s0043-1648(00)00382-3
[23] J. Goddard, H. Wilman, Wear, *5*(2) (1962)114-135;
https://doi:10.1016/0043-1648(62)90235-1
[24] Z. Q. Liu, J. Sun, W.D. Shen. Tribol Int.*35*(8) (2002)511-522;
https://doi:10.1016/s0301-679x(02)00046-4
[25] Z. Yang, Z. Zhang, Y.N. Chen, Q.Y. Zhao, Y.K. Xu, F.Y. Zhang, H.F. Zhan, S.P. Wang, H.Z. Li, J.M. Hao, Y.Q. Zhao, Scripta Materialia, 211(2022)114493;
https://doi.org/10.1016/j.scriptamat.2021.114493